Sonochemical preparation of Ag_2O–PVA nanocomposites: study on pertinent structural and optical properties and exploring the effect of gamma and neutron irradiation

B. Behmanesh[1], D. Rezaei-Ochbelagh[2], Y. Azizian-Kalandaragh[1,3,*] and Gh. Imanzadeh-Karkaragh[4]

[1]Department of Physics, University of Mohaghegh Ardabili, Ardabil, Iran
[2]Department of Nuclear Engineering and Physics, Amirkabir University of Technology, Tehran, Iran
[3]Department of Engineering Sciences, Sabalan University of Advanced Technologies (SUAT), Namin, Iran
[4]Department of Chemistry, University of Mohaghegh Ardabili, Ardabil, Iran

In the paper, Ag_2O–PVA nanocomposites have been prepared by ultrasound-assisted method and the effect of gamma and neutron irradiation has been studied on their optical and structural properties. X-ray diffraction patterns and thermogravimetric analyses also confirm the formation of silver oxide nanoparticles in polyvinyl alcohol polymer. The optical changes in the samples induced by gamma and neutron irradiation were revealed through Fourier transform infrared and diffusive reflectance spectroscopy. Surface morphology of the as-prepared, irradiated and non-irradiated samples has been studied by scanning electron microscopy. The results confirm the observed changes in both optical and structural properties.

Keywords: Ag_2O–PVA nanocomposites, FT-IR, neutron and gamma irradiation, XRD.

OVER the last decades, considerable scientific and technological interests have been focused on nanosized metal-polymer composite materials due to their size-dependent properties and potential applications[1,2].

Among different metal nanostructures, silver and its compounds in different forms are important materials, and cover a wide area of applications in nonlinear optics, biology and medicine, tunable surface plasmon absorption, optoelectronics and nanoelectronics[3–8].

Various techniques have been reported for preparation of Ag-based nanostructures and nanocomposite materials such as radiolytic synthesis[9], atom beam co-sputtering[10], evaporation–condensation, laser ablation[11], micro-emulsion techniques[12], UV- and microwave initiated reduction[13,14], gamma irradiation[15], electron irradiation[16], chemical reduction of inorganic and organic reducing agents[17], and thermal decomposition of silver oxalate in water and in ethylene glycol[18] methods. Recently, ultrasonic waves have been used to prepare different types of nanostructures[19]. A wide range of nanomaterials were obtained using the sonochemical method, such as metals, alloys, metal oxides, metal sulphides, metal nitrides, metal-polymer composites and so on. Several studies have earlier discussed the preparation of silver oxide nanoparticles and a few reports have been presented on the preparation of Ag-based nanostructures with the sonochemical method[19–23]. Different additives are usually incorporated in polymer to modify and improve its properties. Inorganic additives such as transition metal salts have a considerable effect on the optical and electrical properties of polyvinyal alcohol (PVA)[24]. A number of organic materials are known as protective agents for preventing silver particle coalescence[25]. PVA is a semi-crystalline polymer[26,27] that has important applications due to the role of OH groups and hydrogen bonds[28]. PVA is easily soluble in the polar solvent such as water, so it is the best option for nanoparticle synthesis. Undesirable properties of PVA, such as poor solvent resistance, insufficient strength and low heat stability, have restricted its further applications. Therefore, to improve its properties, it is used as a blend form (composite of polymer-metal nanoparticles)[29–32]. Recently, several studies discussed the effect of gamma irradiation on PVA nanocomposites. Omer *et al.*[33] irradiated Ag–PVA nanocomposites by gamma rays and studied the structural and optical properties of nanocomposites. Rishi *et al.*[34] studied the effect of gamma irradiation on the plasmon resonance of Ag–PVA nanocomposites and Uslu *et al.*[35] studied the effect of gamma irradiation on the Schottky barrier diodes (SBDs) fabricated by Au–PVA nanocomposites. Here we report the effect of gamma and neutron irradiation on the structural and optical properties of sonochemically prepared Ag_2O–PVA nanocomposites. The prepared, irradiated and non-irradiated samples have been characterized by X-ray diffraction (XRD), thermogravimetric analyses (TGA),

*For correspondence. (e-mail: yashar.a.k@gmail.com)

diffusive reflectance spectroscopy (DRS) and Fourier transform infrared (FT-IR) spectroscopy.

Materials and methods

Instruments and materials

$Ag(NO_3)_2$ (mol. wt = 169.87 g mol^{-1}), NaOH (mol. wt = 40 g mol^{-1}) and PVA powder were obtained from Merck Co. Deionized water was used throughout the experiment. A high intensity ultrasound processor of Dr Heilscher (UP200H Germany, 14 mm diameter Ti horn, 200 W/cm^2, 24 kHz) was used for preparation of nanostructures. TGA was done by LINSEIS STA-PT 1000. XRD pattern of the products was studied on Philips X'Pert X-ray diffractometer CuKα (λ = 0.154 nm) employing a scanning step of 0.02°S^{-1}, in the 2θ range from 10° to 80°. Surface morphology of Ag_2O–PVA nanocomposite film was studied by LEO 1430 VP scanning electron microscope (SEM) with 15 and 18 kV accelerating voltages. Optical absorption spectra of the samples were measured using DRS (Scinco 4100) spectrophotometer in the wavelength range 190–900 nm. FT-IR was used for KBr supported samples over the wavenumber range 400–4000 cm^{-1} using a FT-IR spectrophotometer (model Varian-3600).

To study the effect of gamma and neutron irradiations, the following sources with given doses and energies have been used:

(i) An Am–Be neutron source with 5.2 Ci activity and of about 7.9×10^{11} (n/cm^2) radiation fluency with doses approximately 1.5 MGy.

(ii) A ^{60}Co (1.17 and 1.13 MeV) gamma source with doses 100 kGy (high dose).

(iii) A ^{137}Cs (0.66 MeV) gamma source with doses of about 10 Gy (low dose).

Preparation of Ag_2O, PVA polymer and Ag_2O–PVA nanostructures

In a typical process, 1.34 g of $Ag(NO_3)_2$ was dissolved in 40 ml doubled distilled water. In another baker of 0.32 g of NaOH was dissolved in 40 ml distilled water. Both the solutions were then mixed and kept under high intensity ultrasonic waves at room temperature for 20 min. After this process, a precipitate of silver oxide was obtained from solution after five times washing using a shaker and centrifuge device. The brown precipitate obtained was dried in open air. Five grams of PVA was dissolved in 95 ml of deionized water at 90°C stirred by a magnet for about 2 h until a clear solution is obtained. The solution was left to cool at room temperature for 2–3 days to obtain a homogeneous solution. Ag_2O powder (3 g) was dissolved in 10 ml of PVA using ultrasonic bath, then 3 ml of Ag_2O–PVA was cast onto a glass substrate and was dried at room temperature for 2 days. Accordingly, the film of Ag_2O–PVA composite was made.

Films of the obtained samples (PVA film, Ag_2O powder, Ag_2O–PVA film) were irradiated for 38 days under Am–Be neutron, and ^{60}Co (1.17 MeV and 1.13 MeV) and ^{137}Cs (0.66 MeV) gamma sources. A piece of the obtained films is used as a reference.

Results and discussion

Structural and morphological characterization

Thermogravimetric analysis (TGA)*:* Thermal degradation of sonochemically prepared silver-based nanostructures to pure Ag_2O nanoparticles was studied using a thermogravimetric analyser (Figure 1). All TGA spectra were recorded in air atmosphere. In this study, first, the aim was to develop a suitable method that could determine the conversion of the as-prepared silver based mixture to Ag_2O and then metallic Ag nanostructures using TGA method. Thermal decomposition of silver-based materials is a complicated process. From the TGA curve (Figure 1) of the silver mixture, the main decomposition steps are: (i) the weight loss at 50–150°C due to moisture vaporization; (ii) decomposition to different phases of crystalline silver oxide from 180°C to 220°C, and finally (iii) a rapid decomposition of silver oxide to metallic Ag at about 400°C. TGA was measured on Ag_2O–PVA, gamma-irradiated PVA (100 kGy), gamma-irradiated PVA (~10 Gy), neutron irradiated PVA and pure PVA (Figure 2). There are meaningful differences between Ag_2O–PVA nanocomposites and pure Ag_2O nanostructures in TGA curves in Figures 1 and 2.

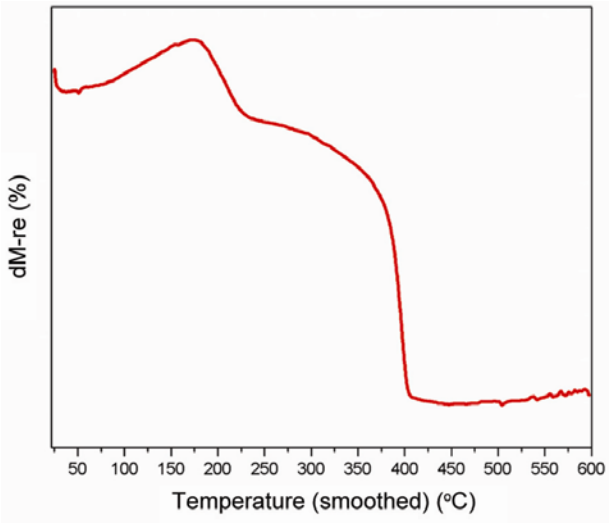

Figure 1. TGA spectrum showing the phase transition of silver hydroxide to silver oxide.

A change in thermal stability of nanocomposite can be seen with the addition of PVA to Ag_2O powder. For instance, the onset of thermal degradation is shifted to higher temperatures by about 100°C for the Ag_2O–PVA nanocomposite. Figure 2 shows that most effects are due to PVA polymer, and the presence of Ag_2O and the effects of irradiations are negligible. Generally, the degradation of polymers starts with free radical formations at weak bonds and or chain ends, followed by their transfer to adjacent chains via inter-chain reactions. The improved thermal stability can be explained through reduced mobility of PVA chains in the nanocomposite. Because of reduced chain mobility, the chain transfer reaction will be suppressed, and consequently the degradation process will be slow and decomposition will take place at higher temperatures. This result indicates that the thermal decomposition routes of pure PVA, Ag_2O–PVA nanocomposites and pure Ag_2O nanopowder are different. We believe that the observed behaviour is most likely the consequence of attachment of the PVA chains to the surface of the Ag_2O nanoparticles (Figures 1 and 2).

The comparison of degradation temperatures for PVA without irradiation, by neutron and gamma irradiation with different doses shows that neutron irradiation has reduced the thermal resistance of PVA slightly, while the thermal resistance of PVA irradiated with various doses of gamma is increased slightly.

Crystalline structure: XRD analysis was performed to study the structural properties of the prepared irradiated and non-irradiated samples. The well-known peak of PVA is obvious in Figure 3. The as-prepared Ag_2O nanoparticles by sonochemical method included Ag_2O phase, a stable phase of silver oxides. In Ag_2O–PVA nanocomposites XRD pattern, all the XRD peaks of Ag_2O are shown with low intensity and are relatively broad. The decrement of peak intensity is due to the addition of PVA. This confirms the semi-crystalline nature of PVA. Some of Ag_2O small peaks also disappear in Ag_2O–PVA diffraction pattern. The most common method of determining the particle size is from the width β (FWHM) of the prominent-ray diffraction (XRD) peaks using Scherrer's formula

$$L = 0.9\lambda/\beta\cos\theta.$$

Here L is the coherent length, λ the wavelength of X-ray radiation and θ is the angle of diffraction. In the case of spherical crystallites, the relation between L and D, the diameter of crystalline, is given by $L = (3/4)D$ (ref. 36). Using Scherrer's formula the nano size of Ag_2O crystallites and Ag_2O–PVA nanocomposites was evaluated and the average nanoparticle sizes calculated to be less than 9 and 15 nm respectively (Figure 3).

Morphological study: Controlling the size and morphology of nanoparticles has a great role in their characteristics and properties. The surface morphology of irradiated and non-irradiated samples has been studied by SEM. Figure 4 *a* shows the SEM image of sonochemically prepared Ag_2O nanostructures, Figure 4 *b* presents the SEM image of the Ag_2O nanostructures irradiated under neutron irradiation. Figure 4 *c* and *d* shows the SEM image of gamma irradiated Ag_2O nanostructures with low and high dose irradiations respectively.

A comparative study of these images shows that in all cases nanoparticles are formed in a polydispersive spherical nanoclusters. A comparison between the figures shows more aggregations in the irradiated nanopowders. A

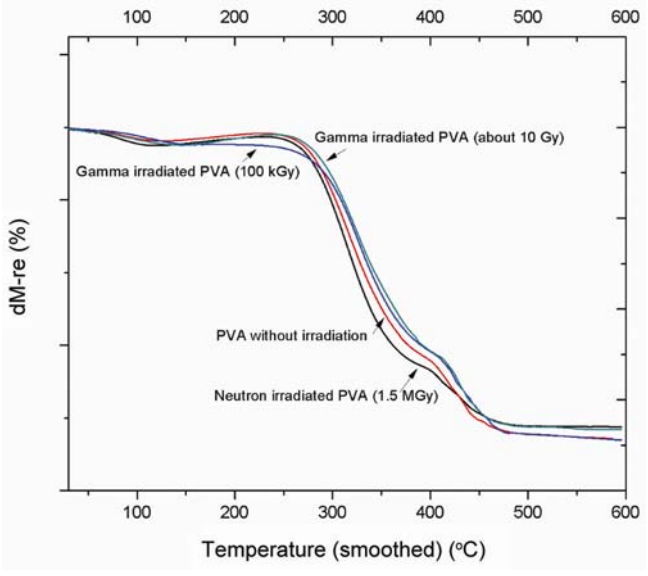

Figure 2. TGA spectra of pure PVA films, without irradiation, irradiated by neutron and gamma with different doses.

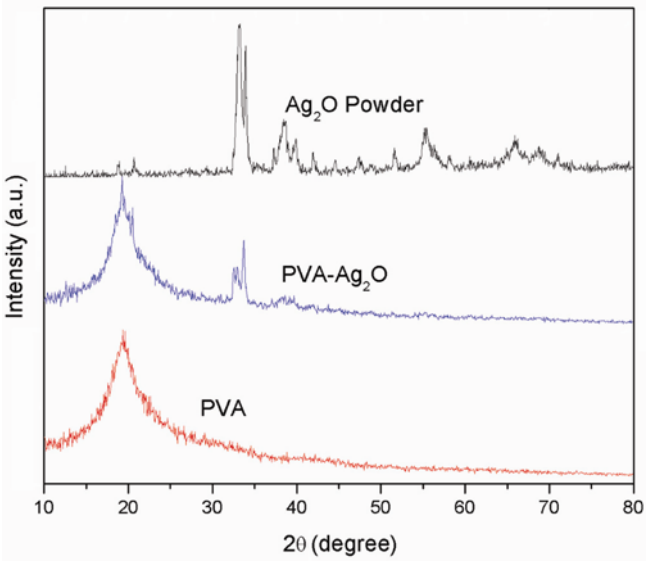

Figure 3. X-ray diffraction of the samples (PVA, Ag_2O, Ag_2O–PVA).

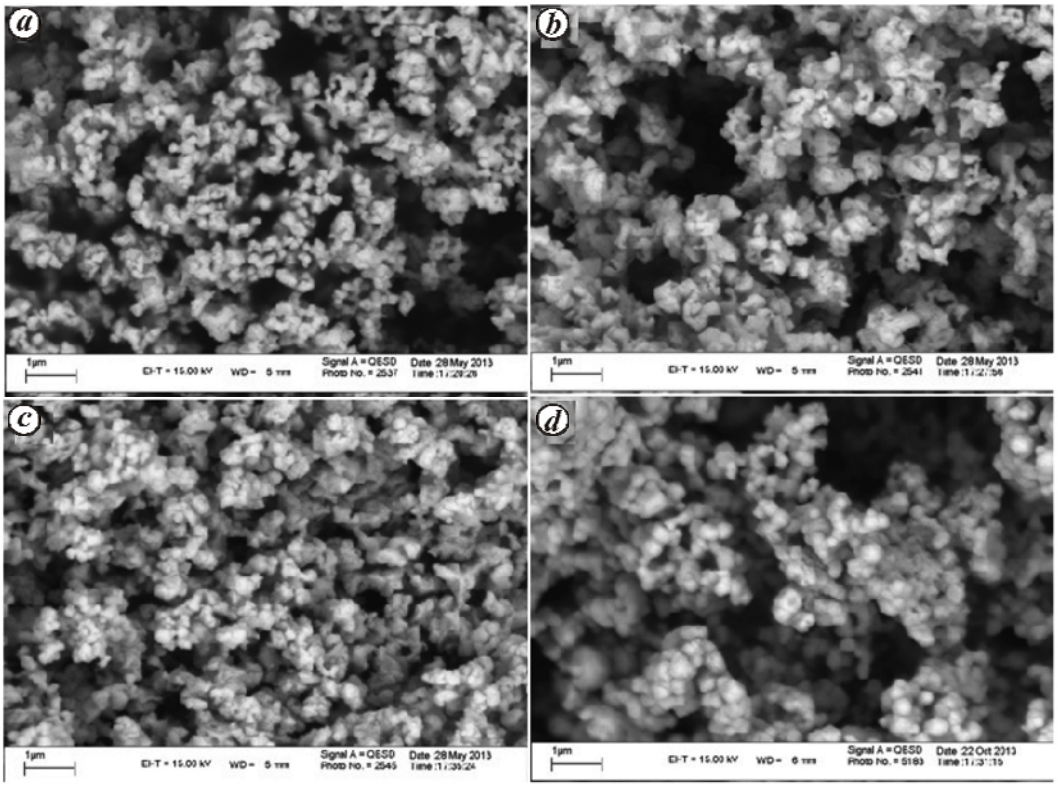

Figure 4. SEM of Ag_2O, without irradiated (***a***), irradiated by neutron (***b***), irradiated by gamma (~10 Gy) (***c***), irradiated by gamma (100 kGy) (***d***).

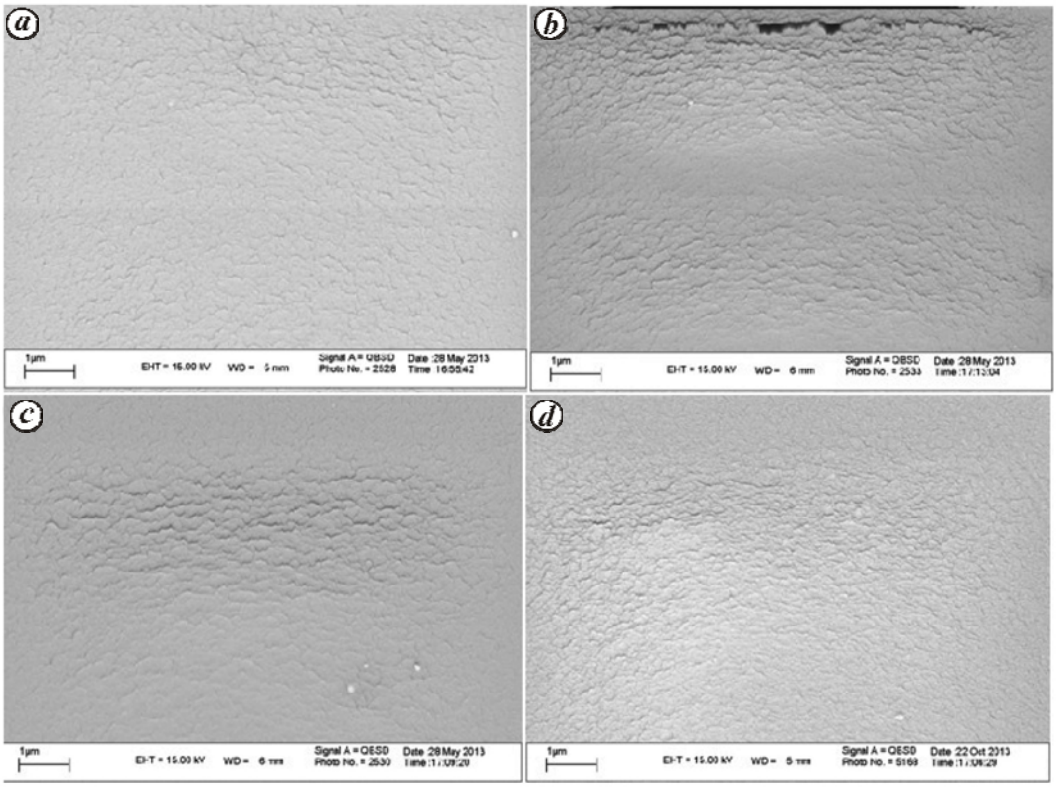

Figure 5. SEM of PVA, without irradiated (***a***), irradiated by neutron (***b***), irradiated by gamma (~10 Gy) (***c***), irradiated by gamma (100 kGy) (***d***).

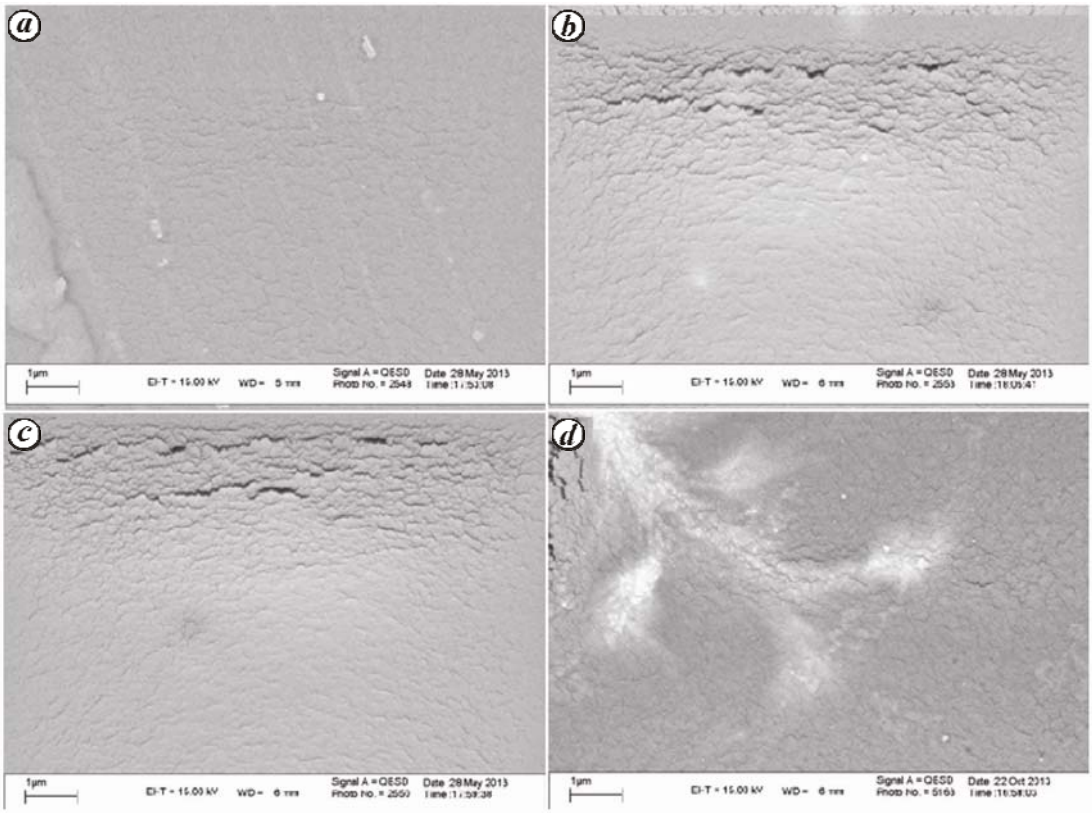

Figure 6. SEM of Ag_2O–PVA, without irradiated (***a***), irradiated by neutron (***b***), irradiated by gamma (~10 Gy) (***c***), irradiated by gamma (100 kGy) (***d***).

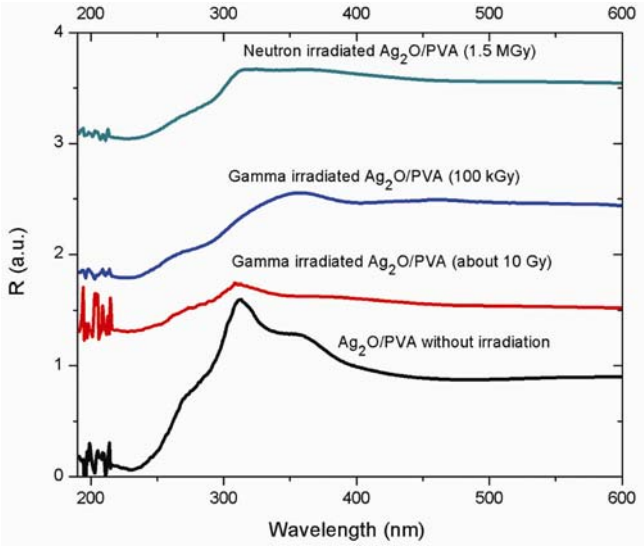

Figure 7. DRS spectra of irradiated and non-irradiated Ag_2O–PVA nanocomposites by neutron and gamma with different doses.

comparative study of Figures 5 and 6 did not show a meaningful difference between surface morphologies of gamma and neutron irradiated samples.

Optical properties of Ag_2O powder, PVA polymer and Ag_2O–PVA nanocomposite films

DRS spectroscopic analysis: Figure 7 shows the DRS spectra of Ag_2O–PVA nanocomposites that irradiated by neutron and gamma at various doses. Comparison of the spectra of nanocomposites indicates that the high dose of gamma radiation (100 kGy) influenced the optical properties of the samples, but gamma radiation with a low dose and neutron (1.5 MGy) did not have a significant effect on peak location. Gamma ray with 100 kGy doses causes peak shifts toward higher wavelengths and there are also changes in peak width due to changes in the distribution of particles (Figure 7)[37].

FT-IR spectroscopy analysis: The transmission spectra of PVA is shown in Figure 8 *a*, *b*. The spectrum obtained from the PVA has an additional peak than the standard spectrum taken from SDBS database (B). This can be attributed to the oxidation of PVA in the air. The additional peak appearing in Figure 8 shows the C=O band formation.

Figure 9 shows the FT-IR spectra of Ag_2O. A comparison between Figure 9 *a* and the spectra taken from SDBS database (B), shows the same bonds. The broad peaks of Ag_2O prepared in this project can be attributed to the presence of water in it.

Figure 10 shows the FT-IR spectra of PVA without irradiation, irradiated by neutron and gamma with different doses. There are C–H, C–O, C=O and O–H bonds in PVA without irradiation. The FT-IR spectra of PVA irradiated with neutron depict changes compared to the non-irradiated PVA. All the peaks are sharper with applying radiation, conveying the regulation of molecular bonds in PVA. However, the PVA irradiated by different doses of gamma rays led to cleavage by chemical bands in PVA, approximately with the same molecular weight. In other words, gamma radiation converted the polymer with different molecular sizes (an impure compound) into a polymer with equal molecular sizes (a pure compound) in the regulation of structural of PVA. The material with regulation structure includes symmetric IR and sharper peaks.

Figure 11 shows the FT-IR spectra of Ag_2O without irradiation, irradiated by neutron and gamma with different doses. Comparison of non-irradiated Ag_2O with Ag_2O irradiated by neutron and gamma rays with different doses shows that neutron (1.5 MGy) and gamma (~10 Gy) radiations had little effect on silver oxide, but did not alter the nature of the material. While a high dose of gamma ray (100 kGy) causes loss of all functional groups, it also changes the nature of the material.

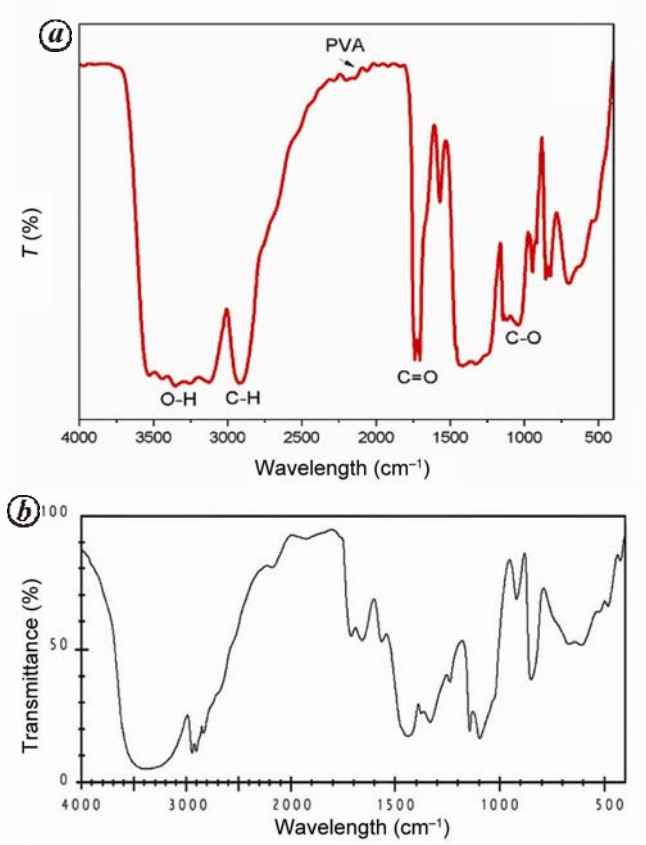

Figure 8. FT-IR spectra of (***a***) prepared PVA and (***b***) obtained PVA from SDBS database.

Figure 12 shows the FT-IR spectra of Ag_2O–PVA without irradiation, irradiated by neutron and gamma rays with different doses. It shows that neutrons and gamma radiations with different doses have little effect on Ag_2O–PVA, so that its peaks are sharper. However, radiations cannot change the nature of Ag_2O–PVA.

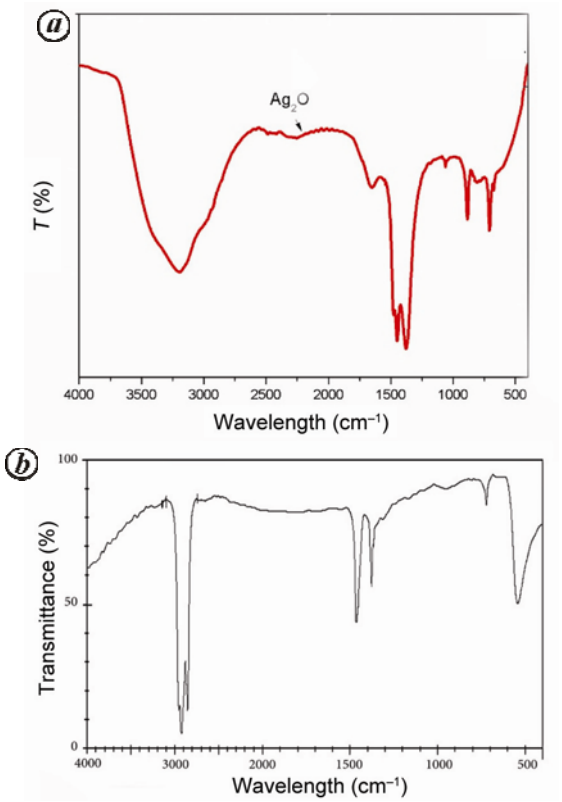

Figure 9. FT-IR spectra of (***a***) prepared Ag_2O and (***b***) obtained Ag_2O from SDBS database.

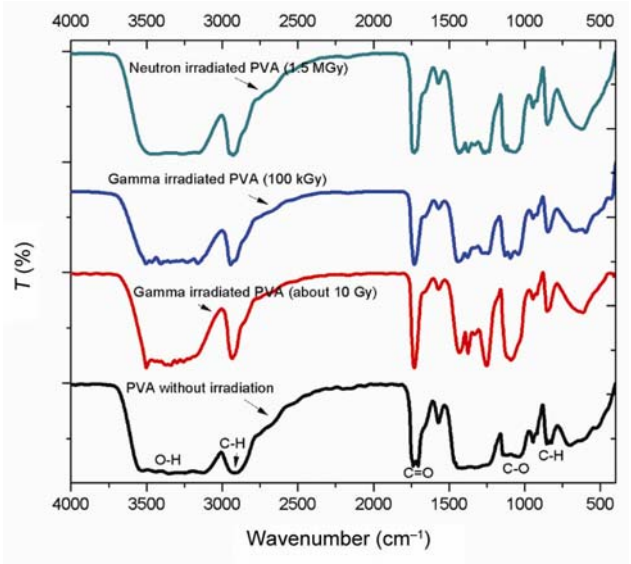

Figure 10. FT-IR spectra of irradiated and non-irradiated PVA films by neutron and gamma with different doses.

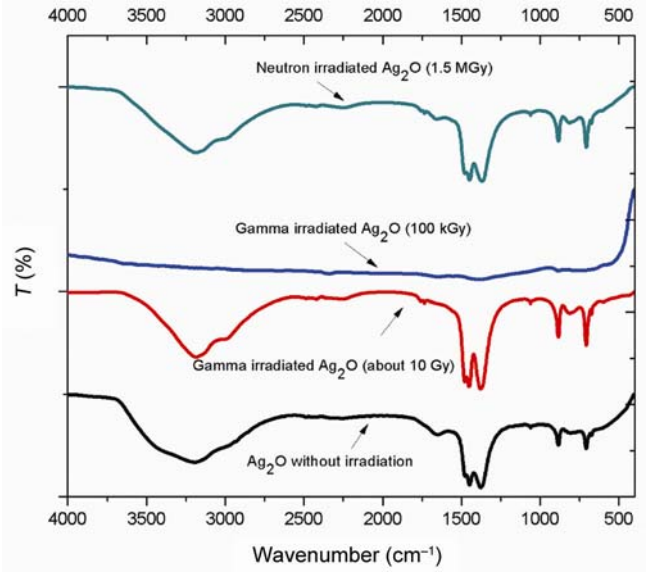

Figure 11. FT-IR spectra of irradiated and non-irradiated Ag_2O powder by neutron and gamma with different doses.

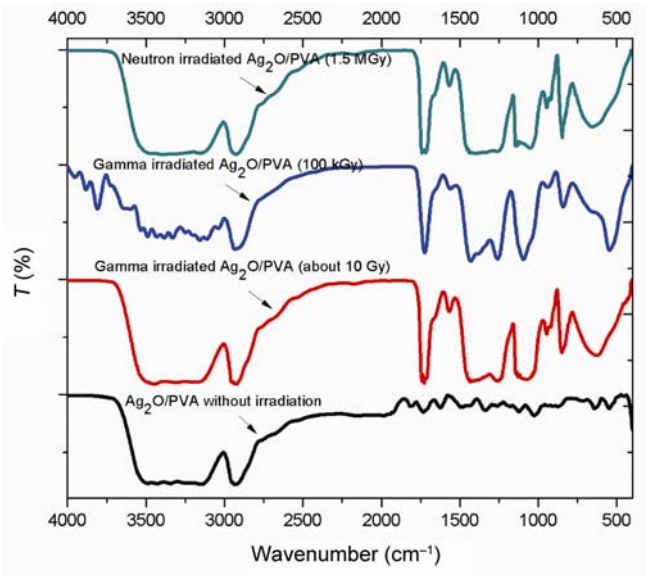

Figure 12. FT-IR spectra of the irradiated and non-irradiated Ag_2O–PVA nanocomposites by neutron and gamma with different doses.

Conclusions

The silver oxide particles were prepared by ultrasonic waves and exposed to neutron and gamma radiations by different doses and were characterized by using DRS, FT-IR spectroscopy, SEM, XRD and TGA. The X-ray diffraction pattern showed that the sizes of Ag_2O and Ag_2O–PVA crystallite are less than 9 and 15 nm. After gamma and neutron irradiation, TGA analysis revealed that the heat resistance of PVA increased with different doses of gamma, while neutron decreased the heat resistance of PVA. SEM images showed that neutron and gamma radiations with different doses had effect on Ag_2O particles. DRS spectra of Ag_2O–PVA showed that high dose of gamma can shift its peak toward higher wavelengths, but neutron and gamma radiations with low dose did not have a significant effect on the peak location. The FT-IR spectra of the neutron and gamma irradiated PVA show greater regularity in its structure. An important point in FT-IR spectra of Ag_2O is that the high dose of gamma ray alters the nature of the material.

1. Avasthi, D. K., Mishra, Y. K., Kabiraj, D., Lalla, N. P. and Pivin, J. C., Synthesis of metal–polymer nanocomposite for optical applications. *Nanotechnology*, 2007, **18**, 125604.
2. Faupel, F., Zaporojtchenko, V., Strunskus, T. and Elbahri, M., Metal-polymer nanocomposites for functional applications. *Adv. Engg. Mater.*, 2010, **12**(12), 1177–1189.
3. Khanna, P. K. *et al.*, Synthesis and characterization of Ag/PVA nanocomposites by chemical reduction method. *Mater. Chem. Phys*., 2005, **93**, 117–121.
4. Temgire, M. K. and Joshi, S. S., Optical and structural studies of silver nanoparticles. *Radiat. Phys. Chem*., 2004, **71**, 1039–1044.
5. Avasthi, D. K. *et al.*, Synthesis of plasmonic nanocomposites for diverse applications. *J. Nanosci. Nanotechnol*., 2010, **10**, 2705–2712.
6. Sharma, V. K., Yngard, R. A. and Lin, Y., Silver nanoparticles: green synthesis and their antimicrobial activities. *Adv. Colloid. Interf. Sci*., 2009, **145**, 83–96.
7. Mishra, Y. K. *et al.*, Controlled reduction of size of Ag nanoparticles embedded in teflon matrix by MeV ion irradiation. *Nucl. Instrum. Meth. Phys. Res. B*, 2008, **266**, 1804–1809.
8. Krklje, A., Nedeljkovi, J. and Kaarevi-Popovi, Z., Fabrication of Ag-PVA hydrogel nanocomposite by gamma-irradiation. *Polym. Bull.*, 2007, **58**(1), 271–279.
9. Krklje, A., Marinovi-Cincovo, M., Kaarevi-Popovi, Z. and Nedeljkovi, J., Radiolytic synthesis and characterization of Ag–PVA nanocomposites. *Eur. Polym. J.*, 2007, **43**, 2171–2176.
10. Mishra, Y. K., Mohapatra, S., Chakravadhanula, V. S. K., Lalla, N. P., Zaporojtchenko, V., Avasthi, D. K. and Faupel, F., Synthesis and characterization of Ag-polymer nanocomposites. *J. Nanosci. Nanotechnol.*, 2010, **10**, 2833–2837.
11. Kruis, F., Fissan, H. and Rellinghaus, B., Sintering and evaporation characteristics of gas-phase synthesis of size-selected PbS nanoparticles. *Mater Sci. Eng. B*, 2000, **69**, 329–334.
12. Krutyakov, Y., Olenin, A., Kudrinskii, A., Dzhurik, P. and Lisichkin, G., Aggregativestability and polydispersity of silver nanoparticles prepared using two-phase aqueous organic systems. *Nanotechnol. Russia*., 2008, **3**, 303–310.
13. Huang, H. and Yang, Y., Preparation of silver nanoparticles in inorganic clay suspensions. *Compos. Sci. Technol*., 2008, **68**, 2948–2953.
14. Chen, X. and Schluesener, H. J., Nano-silver: a nanoproduct in medical application. *Toxicol. Lett*., 2008, **176**, 1–11.
15. Long, D., Wu, G. and Chen, S., Preparation of oligochitosan stabilized silver nanoparticles by gamma irradiation. *Radiat. Phys. Chem*., 2007, **76**(7), 1126–1131.
16. Bogle, K. A., Dhole, S. D. and Bhoraskar, V. N., Silver nanoparticles: synthesis and size control by electron irradiation. *Nanotechnology*, 2006, **17**, 3204–3214.
17. Bonnemann, H. and Richards, R., Nanoscopic metal particles – synthetic methods and potential applications. *Eur. J. Inorg. Chem*., 2001, **10**, 2455–2465.
18. Navaladian, S. *et al.*, Thermal decomposition as route for silver nanoparticles. *Nanoscale Res. Lett*., 2007, **2**, 44–54.

19. Manoiu, V. S. and Aloman, A., Obtaining silver nanoparticles by sonochemicalmethods. UPB. *BuletinScientific. Series B*, 2010, **72**, 179–186.
20. Zhu, Y. P., Wang, X. K., Guo, W. L., Wang, J. G. and Wang, C., Sonochemical synthesis of silver nanorods by reduction of silver nitrate in aqueous solution. *Ultrasonic Sonochem.*, 2010, **17**, 675–679.
21. Darroudi, M., Khorsand, A., Muhamad, M. R., Huang, N. M. and Hakimi, M., Green synthesis of colloidal silver nanoparticles by sonochemical method. *Mater. Lett.*, 2012, **66**, 117–120.
22. Wani, I. A., Ganguly, A., Ahmed, J. and Ahmad, T., Silver nanoparticles: ultrasonic wave assisted synthesis, optical characterization and surface area studies. *Mater. Lett*., 2011, **65**, 520–522.
23. Darroudi, M., Ahmad, M. B., Abdullah, A. H. and Ibrahim, N. A., Green synthesis and characterization of gelatin-based and sugar-reduced silver nanoparticles. *Int. J. Nanomed*., 2011, **6**, 569–574.
24. Abdelaziz, M. and Abdelrazek, E. M., Effect of dopant mixture on structural, optical and electro spin resonance properties of polyvinyl alcohol. *Phys. B*, 2007, **390**, 1–8.
25. Puiso, J., Adline, D., Guobiene, A., Prosycevas, I. and Plaipaite-Nalivaiko, R., Modification of Ag-PVP nanocomposites by gamma irradiation. *Mater. Sci. Eng. B*, 2011, **176**, 1562–1565.
26. Takahashi, Y., Neutron structure analysis of poly(vinyl alcohol). *J. Polym. Sci. Part B: Polym. Phys*., 1997, **35**, 193–195.
27. Tawansi, A., Zidan, H. M., Oraby, A. H. and Dorgham, M. E., Short range-order spin clusters in one-dimensional Ising-like antiferromagnetic CBr_2-filled PVA films: a study of physical properties. *J. Phys. D: Appl. Phys*., 1998, **31**, 3428–3436.
28. Pacansky, J. and Schneider, S., Electron beam chemistry in solid films of poly(vinyl alcohol): exposures under vacuum and under nitrogen at atmospheric pressure; irradiation monitored using infrared spectroscopy. *J. Phys. Chem*., 1990, **94**, 3166–3173.
29. Chang, J. H., Jang, T. G., Ihn, K. J. and Sure, G. S., Poly(vinyl alcohol) nanocomposites with different clays: pristine clays and organoclays. *J. Appl. Polym. Sci*., 2003, **90**, 3208–3216.
30. Yu, Y. H., Lin, C. Y., Yeh, J. M. and Li, W. H., Preparation and properties of poly(vinyl alcohol)-clay nanocomposite material. *Polymer*, 2003, **44**, 3553–3560.
31. Podsiadlo, P. *et al*., Ultrastrong and stiff layered polymer nanocomposites. *Science*, 2007, **318**, 80–83.
32. Sapalidis, A. A., Katsaros, F. K., Romanos, G. E., Kakizis, N. K. and Kanellopoulos, N. K., Preparation and characterization of novel poly-(vinyl alcohol)-zostera flakes composites for packaging applications. *Compos. Part B: Eng.*, 2007, **38**, 398–404.
33. Omer, M. A., Saion, E., Gar-Elnabi, M. E. M., Balla, E. A. A., Dahlan, K. M. and Yousif, Y. M., Gamma radiation synthesis and characterization of polyvinyl alcohol/silver nanocomposites film. *J. Sci. Technol*., 2011, **12**(1), 104–110.
34. Rishi, P. C., Suman, M., Tomar, A. K. and Shyam, K., γ-Irradiated PVA/Ag nanocomposite films: materials for optical applications. *J. Alloys Compounds*, 2012, **538**, 212–219.
35. Uslu, H., Yıldırım, M., Altındal, S. and Durmus, P., The effect of gamma irradiation on electrical and dielectric properties of organic-based Schottky barrier diodes (SBDs) at room temperature. *Radiat. Phys. Chem.*, 2012, **81**, 362–369.
36. Mathew, X., Does the band gap calculated from the photocurrent of Schottky devices lead to erroneous results? Analysis for CdTe. *J. Phys. D: Appl. Phys*., 2000, **33**, 1565–1571.
37. Eisa, W. H., Abdel-Moneam, Y. K., Shaaban, Y., Abdel-Fattah, A. A. and AbouZeid, A. M., Gamma-irradiation assisted seeded growth of Ag nanoparticles within PVA matrix. *Mater. Chem. Phys*., 2011, **128**, 109–113.

Received 29 April 2016; revised accepted 21 August 2016

doi: 10.18520/cs/v112/i04/735-742